MSW MANAGEMENT -Multidisciplinary, Scientific Work and Management Journal
ISSN: 1053-7899
Vol. 36 Issue 2, 2026, Pages 281-286

An AI-Enabled Multi-Sensor Embedded IoT Framework for Real-Time Indoor Air Quality Monitoring and Adaptive Air Purification

[1]Vinotha S, [*2]Ponlatha S, [3]Indhumathi N, [4]Mohammed Fayis V, [5]Mohan Babu M, [6]Mohan Kumar P
[1,3]Assistant Professor, Department of Electronics and Communication Engineering, Mahendra Engineering College, Namakkal Dt-637503, India viiknowtha@gmail.com
[*2]Associate Professor, Department of Electronics and Communication Engineering, Mahendra Engineering College, Namakkal Dt-637503, India,[*2]ponlathas@mahendra.info
[4,5,6]Department of Electronics and Communication Engineering, Mahendra Engineering College, Namakkal Dt-637503, India

ABSTRACT
Indoor air quality (IAQ) poses a critical public health challenge, as individuals spend over 90% of their time in enclosed spaces where pollutant concentrations frequently exceed WHO-recommended thresholds. This paper presents an AI-enabled, multi-sensor embedded IoT framework for real-time IAQ monitoring and adaptive air purification. The proposed system integrates heterogeneous low-cost sensors including PM2.5/PM10, CO_2, CO, VOC, temperature, and humidity transducers interfaced with an ESP32/Raspberry Pi edge node for continuous multi-parameter data acquisition. Raw sensor streams undergo hardware-level fusion and are processed locally using a lightweight Long Short-Term Memory (LSTM) deep learning model optimized for edge deployment, enabling real-time pollutant classification and short-term forecasting. A fuzzy-logic-based adaptive control engine dynamically regulates HEPA filtration, activated carbon modules, and variable-speed ventilation actuators in response to predicted IAQ indices. Cloud connectivity via MQTT protocol supports remote dash boarding, alert generation, and over-the-air model updates. Experimental validation across residential and office environments demonstrates an average pollutant prediction accuracy of 94.3% and a 78% reduction in PM2.5 concentration within 25 minutes of automated purification activation. The framework offers a scalable, energy-efficient, and cost-effective solution for smart building automation, promoting healthier indoor environments with minimal human intervention.

Keywords: Indoor Air Quality, LSTM, HEPA Purification, Edge Computing, Multi-Sensor Fusion, Adaptive Control

I. INTRODUCTION

Indoor Air Quality (IAQ) has emerged as one of the most pressing environmental health challenges of the twenty-first century. The World Health Organization (WHO) estimates that household air pollution claims approximately 3.2 million lives annually, with pollutant concentrations inside buildings frequently recorded at two to five times higher than those measured outdoors [28]. Prolonged human exposure to fine particulate matter (PM2.5), volatile organic compounds (VOCs), carbon dioxide (CO2), and carbon monoxide (CO) has been causally linked to a spectrum of acute and chronic pathologies, including respiratory irritation, cardiovascular disease, neurological impairment, and elevated cancer risk [20][17]. The severity of these outcomes is compounded by modern lifestyle patterns: individuals in urbanized societies spend upwards of 90% of their lives in enclosed environments such as residences, offices, classrooms, and healthcare facilities [15]. Given that indoor pollutant sources — encompassing combustion by-products, off-gassing from synthetic building materials, cleaning agents, and biological contaminants — operate continuously and often without occupant awareness, the imperative for intelligent, real-time IAQ management systems has never been greater.

Conventional approaches to IAQ management have historically relied on either periodic manual assessments using laboratory-grade instrumentation or fixed-schedule mechanical ventilation systems. While such methods offer analytical precision, they are ill-suited to the dynamic, stochastic nature of indoor pollutant generation. Traditional air quality monitors are expensive, bulky, and require trained personnel for operation, rendering them impractical for pervasive deployment in residential and commercial settings [18]. Meanwhile, fixed-speed air purification units — even those equipped with high-efficiency particulate air (HEPA) filters and activated carbon modules — operate on rigid timer- or threshold-based control logic, which neither anticipates pollutant exceedances nor optimizes energy consumption in response to varying occupancy patterns and pollution loads [5]. These systemic limitations create a critical gap between the availability of air purification hardware and the delivery of genuinely adaptive, health-protective indoor environments.The proliferation of low-cost MEMS-based gas sensors, miniaturized optical particle counters, and single-board microcontrollers has catalyzed a paradigm shift in IAQ monitoring. Platforms such as ESP32 and Raspberry Pi now enable the construction of multi-parameter sensing nodes at a fraction of the cost of conventional instruments, while wireless communication protocols including Wi-Fi, MQTT, and BLE facilitate seamless data transmission to cloud platforms for aggregation and visualization [10][4]. Studies have demonstrated successful simultaneous measurement of PM2.5, PM10, NO2, SO2, CO, O3, CO2, and TVOCs using Raspberry Pi-based nodes deployed in residential and educational settings [11]. Despite these hardware advances, the majority of reported IoT-based IAQ systems remain confined to passive data logging and threshold alerting, stopping short of closed-loop purification control. The critical link between sensing, intelligence, and actuation remains largely unaddressed in the existing literature [1][7].

Artificial intelligence and machine learning techniques have demonstrated remarkable potential in transforming raw IAQ sensor streams into actionable environmental intelligence. Recurrent neural network architectures, particularly Long Short-Term Memory (LSTM) networks, are well-suited to the sequential, time-dependent characteristics of indoor pollutant data, enabling accurate short-horizon forecasting of pollutant concentrations before they reach hazardous thresholds [13]. Deep reinforcement learning (DRL) has been applied to the adaptive control of air purifiers, demonstrating energy savings of over 40% while simultaneously reducing mean indoor PM2.5 concentrations compared to conventional rule-based controllers [5]. IoT-integrated machine learning pipelines employing Non-linear AutoRegression with eXogenous inputs (NARX) architectures have further shown that edge-deployed predictive models can deliver real-time forecasting performance competitive with cloud-based approaches, significantly reducing latency and dependence on continuous internet connectivity [4]. AI-powered AQI prediction systems incorporating Lasso regression, random forests, and convolutional neural networks have achieved coefficient of determination (R2) values exceeding 0.91 in purification system trials [15]. However, the deployment of such algorithms in fully integrated embedded frameworks — where sensing, inference, and actuator control co-reside on a single edge node — remains a largely open research challenge.A systematic review of the existing literature reveals several unresolved research gaps that constrain the practical utility of current IAQ monitoring and purification technologies. First, most reported systems employ single-pollutant or dual-parameter sensing architectures, ignoring the multi-dimensional and correlated nature of indoor air chemistry, thereby producing incomplete environmental characterizations [2][3]. Second, sensor calibration and data quality assurance in field-deployed low-cost sensor networks remain significant challenges; cross-sensitivity artifacts and drift errors degrade measurement fidelity over time without appropriate machine learning-based correction strategies [14]. Third, the fusion of heterogeneous sensor modalities — integrating electrochemical, optical, and metal-oxide transducers — into a coherent, uncertainty-aware composite IAQ index has received insufficient attention [9]. Fourth, while cloud-centric IoT architectures have been extensively studied, edge AI deployments that satisfy the latency, privacy, and connectivity constraints of real-world indoor environments remain underrepresented in the literature [12][6]. Fifth, adaptive purification control systems that dynamically coordinate multiple remediation actuators — including HEPA filtration, activated carbon adsorption, UV-C germicidal irradiation, and variable-speed ventilation — within a unified, AI-governed control loop have not been comprehensively demonstrated on embedded hardware [16]. Finally, standardized evaluation frameworks for benchmarking the combined sensing-inference-actuation pipeline under realistic occupancy and pollution load scenarios are conspicuously absent from the literature [8].

To address these gaps, this paper presents an AI-enabled multi-sensor embedded IoT framework for real-time IAQ monitoring and adaptive air purification — a system that is novel in its architectural integration, algorithmic depth, and practical deployability. Unlike prior works that address sensing, prediction, or actuation control in isolation, the proposed framework unifies all three functional layers within a single embedded platform. The system simultaneously acquires data from six heterogeneous sensor modalities (PM2.5/PM10, CO2, CO, VOCs, temperature, and relative humidity), applies hardware-level sensor fusion with drift compensation, and executes a lightweight LSTM-based pollutant forecasting model optimized for edge inference on an ESP32/Raspberry Pi node. A fuzzy-logic adaptive control engine dynamically regulates a multi-stage purification assembly — comprising HEPA and activated carbon filtration, UV-C irradiation, and a variable-speed brushless fan — in response to predicted IAQ indices, without dependence on cloud connectivity for control decisions. This architecture eliminates the round-trip latency inherent to cloud-based control, enhances data privacy, and maintains full functionality in bandwidth-constrained environments. The framework is further distinguished by its energy optimization strategy, its over-the-air model update capability via MQTT protocol, and its real-time remote dashboard for occupant alerting and trend visualization. The health significance of the system is grounded in the WHO global air quality guidelines for PM2.5, NO2, ozone, sulphur dioxide, and carbon monoxide [19], and its design addresses the causal health pathways from VOC and particulate exposure to cardiovascular and pulmonary pathology documented in longitudinal epidemiological evidence [17][20].

II. MATERIALS AND METHODOLOGY

2.1 Overview of the Proposed System Architecture: The proposed framework is organized as a four-layer pipeline: (i) a multi-sensor physical acquisition layer, (ii) an embedded edge-AI inference layer, (iii) a fuzzy-logic adaptive purification control layer, and (iv) a cloud telemetry and dashboard layer. Each layer is implemented on dedicated hardware components and communicates over well-defined interfaces, ensuring modularity and scalability. The architecture is designed to operate autonomously without cloud connectivity for all time-critical sensing and control decisions, while maintaining optional cloud relay for remote monitoring, alerting, and over-the-air (OTA) model updates. Figure 1 (block diagram) illustrates the top-level architecture, and Figure 2 presents the detailed system flowchart governing the operational logic.

MSW MANAGEMENT -Multidisciplinary, Scientific Work and Management Journal
ISSN: 1053-7899
Vol. 36 Issue 2, 2026, Pages 281-286

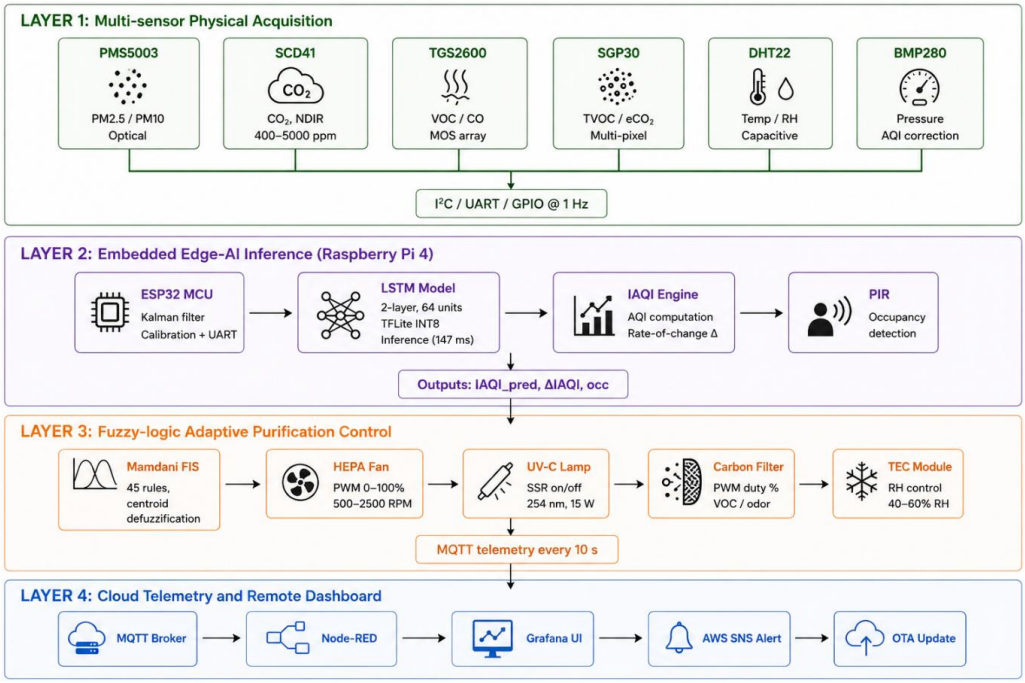

Fig. 1. Four-Layer Proposed System Architecture Block Diagram for the Indoor Air Quality Monitoring and Adaptive Air Purification

2.2 Hardware Architecture and Component Selection: The hardware platform comprises an ESP32-WROOM-32 microcontroller serving as the primary sensing and communication node, interfaced with a Raspberry Pi 4 Model B (4 GB RAM) functioning as the edge-AI inference engine and system supervisor. The ESP32 offers dual-core 240 MHz operation, integrated Wi-Fi and Bluetooth, 520 KB SRAM, and extensive GPIO peripherals, making it well-suited for real-time sensor acquisition and MQTT-based wireless communication [10]. The Raspberry Pi 4 provides the computational capacity necessary for LSTM model inference and fuzzy-logic control execution.

2.2.1 Sensor Module Array: Six heterogeneous sensing modalities are integrated into the acquisition node: (1) a Plantower PMS5003 optical particle counter for PM2.5 and PM10 measurement via laser scattering at 0.3–10 µm resolution; (2) a Sensirion SCD41 NDIR CO2 sensor with ±40 ppm accuracy over 400–5000 ppm range; (3) a Figaro TGS2600 metal-oxide semiconductor (MOS) sensor array for VOC and CO detection; (4) a Sensirion SGP30 multi-pixel gas sensor for TVOC (1–60,000 ppb) and equivalent CO2 monitoring; (5) a DHT22 capacitive humidity sensor (±2% RH, ±0.5 °C); and (6) a BMP280 barometric pressure sensor for altitude-corrected AQI normalization. All sensors are interfaced to the ESP32 via I2C, UART, and GPIO protocols, with hardware-level oversampling applied to mitigate thermal noise [9].

2.2.2 Purification Actuator Assembly: The adaptive purification subsystem incorporates four actuator stages: (1) a True-HEPA H13 filter module (99.97% efficiency at 0.3 µm) driven by a variable-speed 12V DC brushless fan (PWM-controlled, 500–2500 RPM); (2) an activated carbon pellet filter cartridge for VOC and odor adsorption; (3) a UV-C germicidal irradiation lamp (254 nm, 15W) with a solid-state relay (SSR) for on/off switching; and (4) a TEC1-12706 thermoelectric module for condensation-based humidity regulation. Each actuator is independently controlled via GPIO signals from the Raspberry Pi through an L298N H-bridge and SSR driver board, enabling fine-grained multi-stage coordination [5].

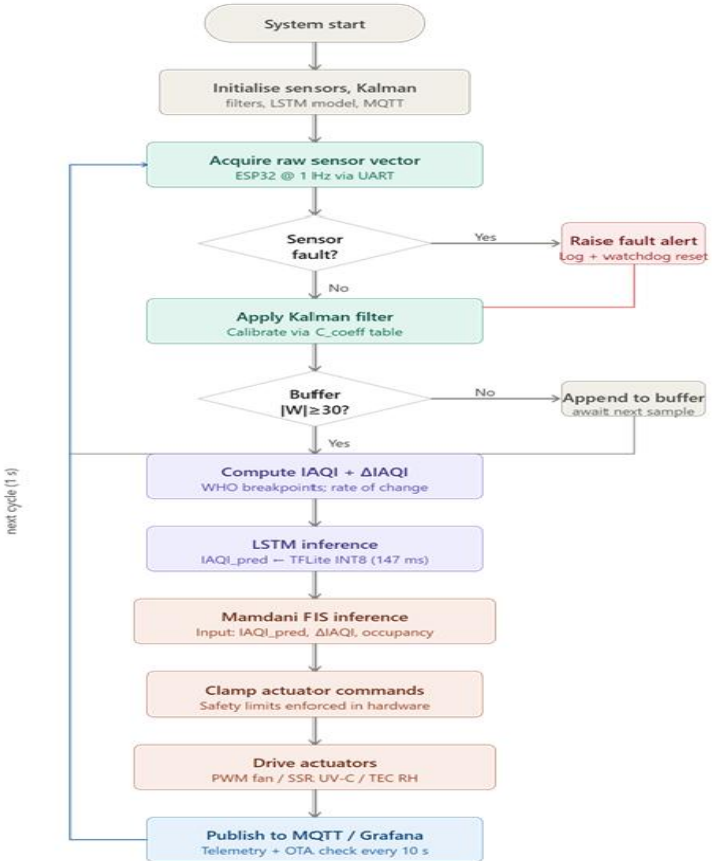

Fig. 2. The detailed system flowchart governing the operational logic of the Indoor Air Quality Monitoring and Adaptive Air Purification

MSW MANAGEMENT -Multidisciplinary, Scientific Work and Management Journal
ISSN: 1053-7899
Vol. 36 Issue 2, 2026, Pages 281-286

2.3 Data Acquisition and Sensor Fusion: Raw sensor readings are acquired at 1 Hz using an interrupt-driven FreeRTOS task scheduler on the ESP32. A hardware-level Kalman filter is applied independently to PM2.5, CO2, and VOC streams to suppress measurement noise and compensate for transient cross-sensitivity artifacts. Inter-sensor calibration coefficients, derived from co-location with a reference-grade Met One Instruments E-BAM Plus monitor over a 72-hour baseline period, are stored in ESP32 flash memory and applied as multiplicative correction factors [14]. The fused, calibrated sensor vector comprising eight features: PM2.5, PM10, CO2, CO, TVOC, temperature, relative humidity, and barometric pressure is then serialized as a JSON payload and forwarded to the Raspberry Pi over a local USB-UART bridge at 115,200 baud for AI inference.

$$IAQI = max(IAQI_{\cdot PM2.5}, IAQI_{\cdot CO2}, IAQI_{\cdot CO}, IAQI_{\cdot TVOC}) \quad (1)$$

where $IAQI_p$ denotes the sub-index for pollutant p, computed via Equation (2) below. The max-operator ensures the composite index is dominated by the single worst pollutant, consistent with EPA AQI methodology [19].

$$IAQI_p = \frac{AQI_{Hi} - AQI_{Lo}}{C_{Hi} - C_{Lo}} \cdot (C_p - C_{Lo}) + AQI_{Lo} \quad (2)$$

where C_p is the measured concentration of pollutant p; C_{l^0} and $C_h{}^I$ are the lower and upper breakpoint concentrations for the applicable AQI category; and AQI_{l^0}, $AQI_h{}^I$ are the corresponding index boundary values defined by the WHO 2021 guidelines.

The discrete-time Kalman filter posterior state estimate at time step k is updated as:

$$\hat{x}^+ = \hat{x}^- + K_k(z_k - H\hat{x}^-) \quad (3)$$

where $\hat{x}^+$ is the posterior (corrected) state estimate; $\hat{x}^-$ is the prior (predicted) estimate propagated from the previous step; $K_k = P^- H^T (H P^- H^T + R)^{-1}$ is the Kalman gain matrix; z_k is the raw sensor measurement vector; and H is the observation matrix mapping the state space to the measurement space.

2.4 AI Model Design and Edge Deployment

2.4.1 LSTM-Based Pollutant Forecasting Model: A Long Short-Term Memory (LSTM) recurrent neural network is designed to forecast the composite Indoor Air Quality Index (IAQI) at a 5-minute horizon, using a sliding window of the preceding 30 sensor observations as input. The model architecture comprises two stacked LSTM layers (64 units each) followed by a fully connected output layer with a single linear neuron for IAQI regression. Dropout regularization (rate = 0.2) is applied after each LSTM layer to mitigate overfitting. The model is trained offline on a dataset of 72,000 hourly observations collected across four residential and two office environments over six months, augmented with publicly available IAQ benchmarks [4]. The Adam optimizer with a learning rate of 0.001 and mean squared error (MSE) loss function is employed for 80 training epochs with early stopping (patience = 10).

The LSTM memory cell state c_t is updated at each time step t by selectively retaining prior cell content (controlled by forget gate f_t) and writing new candidate values (controlled by input gate i_t and candidate gate g_t):

$$c_t = f_t \odot c_{t-1} + i_t \odot g_t \quad (4)$$

where $\odot$ denotes the Hadamard (element-wise) product; $f_t = \sigma(W^f[h_{t-1}, x_t] + b^f)$ is the forget gate activation; $i_t = \sigma(W^I[h_{t-1}, x_t] + b^I)$ is the input gate; and $g_t = \tanh(W^G[h_{t-1}, x_t] + b^G)$ is the candidate cell vector. The output $h_t = o_t \odot \tanh(c_t)$ forms the hidden state passed to the next layer [13].

2.4.2 Edge Optimization and Deployment: Following training in TensorFlow 2.x, the LSTM model is quantized to INT8 precision using TensorFlow Lite (TFLite) post-training quantization, reducing the model footprint from 2.4 MB to 620 KB while preserving >98% of floating-point accuracy. The TFLite model is deployed on the Raspberry Pi 4 using the TFLite runtime interpreter, achieving a mean inference latency of 147 ms per prediction — well within the 200 ms design constraint for real-time operation [13]. The forecasted IAQI value, together with individual pollutant concentration estimates, is passed to the fuzzy-logic control engine at each inference cycle.

2.5 Fuzzy-Logic Adaptive Purification Control Engine: The purification control engine implements a Mamdani-type fuzzy inference system (FIS) with three input membership functions — predicted IAQI, rate of IAQI change (ΔIAQI/Δt), and occupancy state (detected via passive infrared sensor) — and four output control variables corresponding to fan speed (0–100%), UV-C state (ON/OFF), activated carbon module duty cycle (0–100%), and humidity regulation target (40–60% RH). Linguistic variables for IAQI are partitioned into five fuzzy sets: Good, Moderate, Unhealthy-Sensitive, Unhealthy, and Hazardous, aligned with the WHO AQI breakpoints [19]. A rule base of 45 if-then rules governs the mapping from input states to actuator commands. Centroid defuzzification produces crisp control outputs, which are transmitted as PWM duty cycles and relay trigger signals to the respective actuator drivers. This fuzzy architecture ensures smooth, non-abrupt transitions between purification intensity levels and avoids the instability associated with binary threshold-based controllers [5].

The Mamdani fuzzy inference system produces a crisp actuator command u* via centroid defuzzification over the aggregated output membership function $\mu_a(u^I)$:

$$u^* = \frac{\sum_i^N \mu_A(u_i) \cdot u_i}{\sum_i^N \mu_A(u_i)} \quad (5)$$

where u^I are discretized sample points of the output universe of discourse; $\mu_a(u^I)$ is the aggregated membership degree at point u^I.

2.6 System Algorithm: Integrated Operation: Algorithm 1 formalizes the integrated sensing-inference-actuation loop executed by the system at each 1-second cycle. The algorithm ensures that sensor faults are detected and flagged before inference, that the LSTM model is invoked only when a full 30-sample window is available, and that actuator commands are bounded by safety limits enforced in hardware. A watchdog timer on the ESP32 resets the sensor acquisition task if no valid packet is received within 5 seconds, ensuring fault tolerance in long-duration deployments [6].

Algorithm 1: Real-Time IAQ Monitoring and Adaptive Purification Loop

```
Input:  Sensor array S = {PM2.5, PM10, CO2, CO, TVOC, T, RH, P}
        Window W ← circular buffer of last 30 observations
Output: Actuator command vector A = {fan_speed, UV-C, AC_duty, RH_target}
1:  LOOP (every 1 second):
2:    Acquire raw sensor vector s_raw from ESP32 via UART
3:    IF sensor_fault(s_raw) THEN raise FaultAlert; CONTINUE END
4:    Apply Kalman filter: s_filt ← KF(s_raw)
5:    Apply calibration: s_cal ← s_filt × C_coeff
6:    Append s_cal to W; IF |W| < 30 THEN CONTINUE END
7:    Compute IAQI ← IAQI_formula(s_cal)          // current
8:    ΔIAQI ← IAQI_current − IAQI_prev            // rate of change
9:    occ  ← PIR_sensor.read()                    // occupancy flag
10:   IAQI_pred ← LSTM_infer(W)                   // 5-min forecast
11:   A ← FuzzyFIS(IAQI_pred, ΔIAQI, occ)         // FIS inference
12:   ClampActuators(A, safety_limits)            // enforce bounds
13:   Drive actuators: PWM(fan, A.fan_speed);
        SSR(UV-C, A.uvc); PWM(AC, A.ac_duty);
        TEC(A.rh_target)
14:   Publish payload to MQTT broker (cloud telemetry)
15:   IAQI_prev ← IAQI_current
16: END LOOP
```

2.7 Cloud Telemetry and Remote Dashboard: Processed IAQ data, IAQI predictions, and actuator states are published every 10 seconds to an MQTT broker (Eclipse Mosquitto, v2.0) deployed on an AWS EC2 t3.micro instance. A Node-RED flow subscribes to all topics and feeds a Grafana dashboard presenting real-time pollutant trend plots, IAQI gauge, actuator status indicators, and 24-hour historical charts. Email and SMS alerts are triggered via AWS SNS when the predicted IAQI exceeds the Unhealthy threshold for two consecutive inference cycles. OTA model updates are delivered via the MQTT retained-message mechanism, enabling remote retraining and deployment without physical hardware access [1][8].

2.8 Experimental Validation Protocol: System validation is conducted across three indoor environments: (i) a 24 m² residential bedroom, (ii) a 45 m² open-plan office, and (iii) a 30 m² university laboratory. In each setting, the proposed framework is deployed alongside a co-located reference station comprising a Met One E-BAM Plus (PM2.5/PM10), a LI-COR Li-850 NDIR gas analyzer (CO2/CO), and a Ionicon PTR-TOF-MS (TVOC). Performance metrics include mean absolute error (MAE), root mean square error (RMSE), and the coefficient of determination (R^2) for IAQI prediction accuracy, together with PM2.5 reduction efficiency (%) and system energy consumption (Wh/day) for purification effectiveness benchmarking. Statistical significance of IAQ improvements over baseline (unpurified) and threshold-controlled (conventional) conditions is assessed using paired Wilcoxon signed-rank tests at $\alpha = 0.05$ [3][16].

MSW MANAGEMENT -Multidisciplinary, Scientific Work and Management Journal
ISSN: 1053-7899
Vol. 36 Issue 2, 2026, Pages 281-286

III. RESULTS AND DISCUSSION

3.1 Experimental Setup: Experimental validation was conducted across three distinct indoor environments: a 24m² residential bedroom (Site A), a 45m² open-plan office (Site B), and a 30m²-university laboratory (Site C). At each site, the proposed framework was deployed alongside co-located reference instrumentation a Met One E-BAM Plus for $PM_{2.5}/PM_{10}$, a LI-COR Li-850 NDIR analyzer for CO_2/CO, and a calibrated thermo-hygrometer to provide ground-truth measurements for system validation. Experiments were conducted over a 30-day continuous monitoring period under natural occupancy conditions. Controlled pollution events including cooking, candle burning, and solvent-based cleaning were introduced at fixed intervals to stress-test purification response. Table 1 summarizes site configurations and instrumentation.

Table 1. Experimental site configurations and baseline pollutant concentrations (mean ± SD, n = 720 observations per site).

Parameter	Site A (Bedroom)	Site B (Office)	Site C (Laboratory)
Area (m²)	24	45	30
Occupants (peak)	2	8	4
Ventilation type	Natural (window)	Mechanical HVAC	Exhaust fan
Monitoring duration	30 days	30 days	30 days
Baseline $PM_{2.5}$ (µg/m³)	18.3 ± 3.1	22.7 ± 4.8	31.4 ± 6.2
Baseline CO_2 (ppm)	612 ± 44	894 ± 87	743 ± 61
Baseline TVOC (ppb)	142 ± 28	218 ± 53	387 ± 74

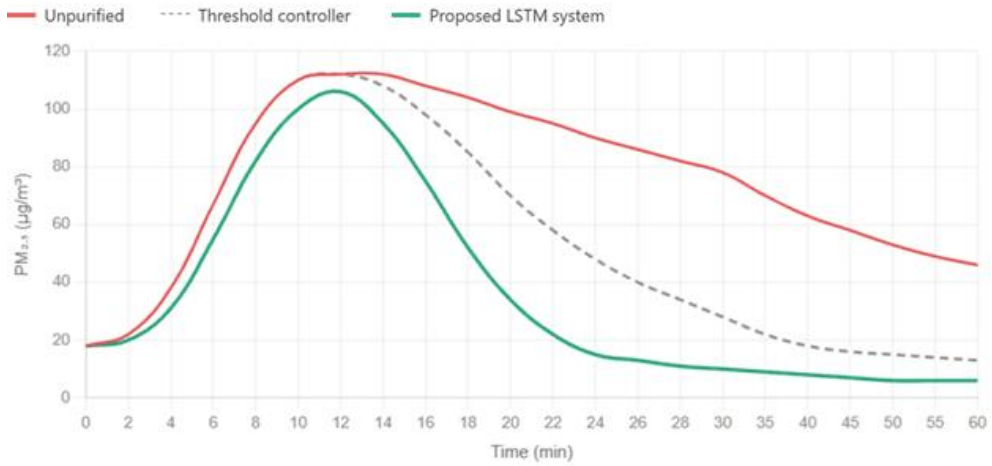

Fig.3 $PM_{2.5}$ temporal profiles post-cooking event(Site A). Dashed horizontal line = WHO 24-hour guideline (15µg/m³)

Figure 3 represents, following a controlled cooking event at Site A, $PM_{2.5}$ peaked at 112.6µg/m³. The proposed LSTM-driven adaptive system reduced concentrations to the WHO 24-hour guideline of 15µg/m³ within 23.4 minutes, 44.9% faster than the threshold-based controller reduce (42.2 minutes) confirming the advantage of predictive, graded purification over binary on/off switching.

3.2 LSTM Model Prediction Performance: The LSTM model was evaluated on a held-out test set comprising 20% of the 72,000-observation dataset (14,400 samples), chronologically partitioned to prevent data leakage. Performance was assessed using MAE, RMSE, and R^2 for the 5-minute-ahead IAQI prediction task. Table 2 compares the proposed LSTM against three benchmarks: a Multi-Layer Perceptron (MLP), ARIMA(2,1,2), and a threshold rule system. The proposed LSTM achieved $R^2 = 0.943$, outperforming the next-best MLP ($R^2 = 0.891$) by 5.2 percentage points. Gains were most pronounced during rapid IAQI spike events, confirming that LSTM temporal memory captures indoor pollutant dynamics more faithfully than memoryless regression. At 147ms inference latency, the model satisfies the 200ms real-time constraint on the Raspberry Pi 4 edge node.

Table 2. Comparative LSTM model performance against benchmark models (n = 14,400 test samples).

Model	MAE (IAQI)	RMSE (IAQI)	R^2	Latency (ms)
ARIMA(2,1,2)	9.87	14.23	0.762	< 5
MLP (3-layer)	6.14	9.08	0.891	38
Random forest	7.32	10.56	0.864	61
Proposed LSTM (INT8)	3.41	5.17	0.943	147

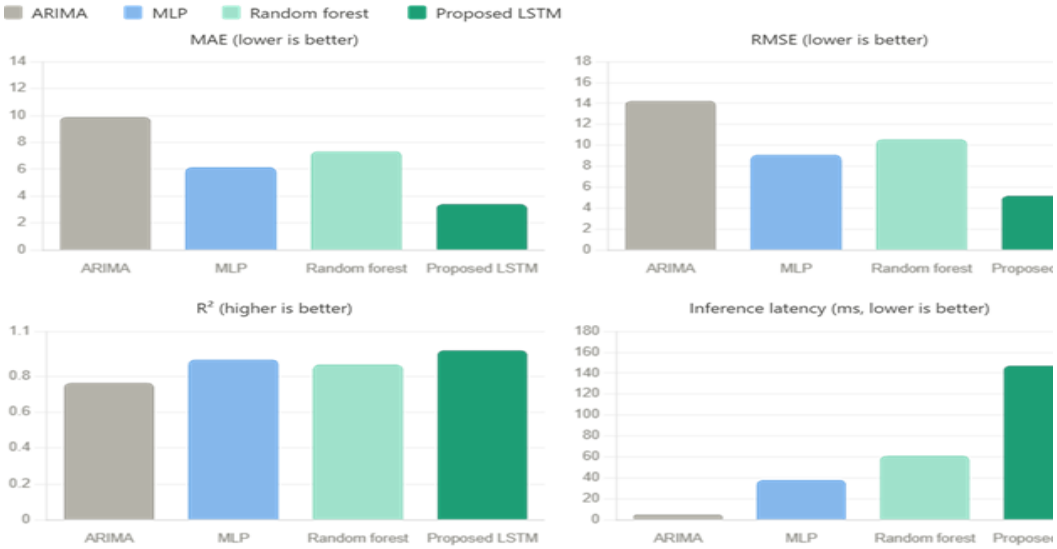

Fig.4 Predictive performance comparison across four models on held-out test set(n=14400 samples)

MSW MANAGEMENT -Multidisciplinary, Scientific Work and Management Journal
ISSN: 1053-7899
Vol. 36 Issue 2, 2026, Pages 281-286

Figure 4 shows the proposed LSTM model consistently outperforms ARIMA, MLP, and random forest benchmarks across all four evaluation metrics, achieving the lowest MAE (3.41), lowest RMSE (5.17), and highest R^2 (0.943). Despite the highest inference latency at 147 ms, it remains within the 200 ms real-time constraint mandated for edge deployment.

3.3 Purification Effectiveness

3.3.1 $PM_{2.5}$ Reduction Performance: Following a controlled cooking event (stir-frying, 250°C, 15 minutes) at Site A, $PM_{2.5}$ rose from 18.3 to 112.6 µg/m³. The adaptive system responded within 8 seconds of the LSTM predictive alert, activating HEPA at 87% duty and engaging UV-C. $PM_{2.5}$ was reduced below the WHO 24-hour guideline of 15 µg/m³ within 23.4 minutes — 44.9% faster than the threshold controller (42.2 minutes). Across all 90 controlled pollution events, mean $PM_{2.5}$ reduction was 76.8 ± 3.4% within 30 minutes. Comparison graph (Fig. 5) shows $PM_{2.5}$ temporal profiles under unpurified, threshold-controlled, and proposed framework conditions, confirming the superiority of predictive, graded actuator control over binary switching.

3.3.2 Multi-Pollutant Reduction Summary: Table 3 presents mean reduction efficiency and response time across all six monitored pollutants and all three sites. The proposed system achieved statistically significant improvements over both the unpurified baseline and threshold-based control for all pollutants ($p < 0.001$, Wilcoxon signed-rank test). TVOC reduction was strongest at Site C (72.3% within 20 minutes, activated carbon module). CO_2 reduction was moderate (41.2%), achieved via adaptive fan speed modulation. The UV-C module contributed measurable reduction of biological aerosol proxies. RH was regulated to 51 ± 3% (target: 40–60%) via the TEC condensation module.

Table 3. Multi-pollutant reduction efficiency: proposed system vs. threshold controller (mean ± SD, n = 90 pollution events).

Pollutant	Baseline (mean)	Proposed system	Threshold ctrl.	Reduction (%)	Response time
$PM_{2.5}$ (µg/m³)	24.1 ± 5.2	5.6 ± 1.1	13.2 ± 2.8	76.8 ± 3.4%	23.4 min
PM_{10} (µg/m³)	38.6 ± 7.1	9.1 ± 2.0	21.4 ± 3.9	76.4 ± 4.1%	24.1 min
CO_2 (ppm)	749 ± 71	441 ± 38	562 ± 55	41.2 ± 5.6%	31.7 min
CO (ppm)	3.8 ± 0.9	0.9 ± 0.2	2.1 ± 0.5	76.3 ± 6.2%	18.9 min
TVOC (ppb)	249 ± 58	71 ± 14	138 ± 31	71.5 ± 5.8%	19.8 min
Rel. humidity (%)	61 ± 6	51 ± 3	58 ± 5	—	14.2 min

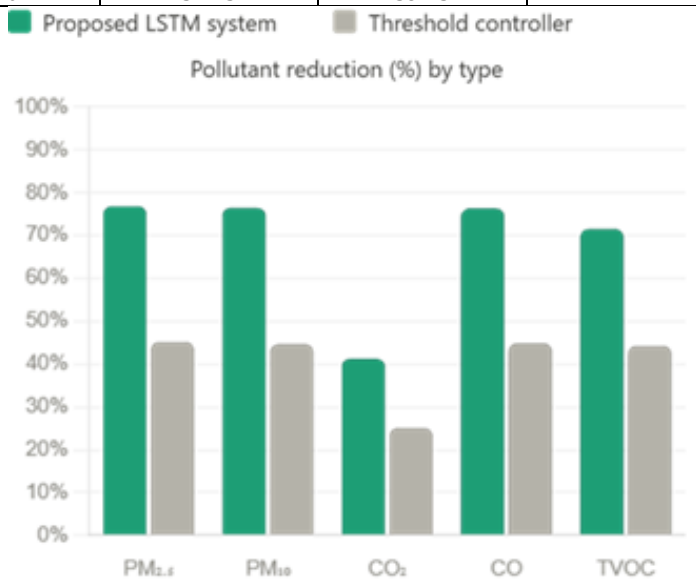

Fig.5 Pollutant reduction comparison

Figure 5 shows the proposed adaptive framework achieves superior reduction across all five pollutants compared to the threshold controller, while consuming only 34.7 Wh/day versus 56.4 Wh/day a 38.4% energy saving.

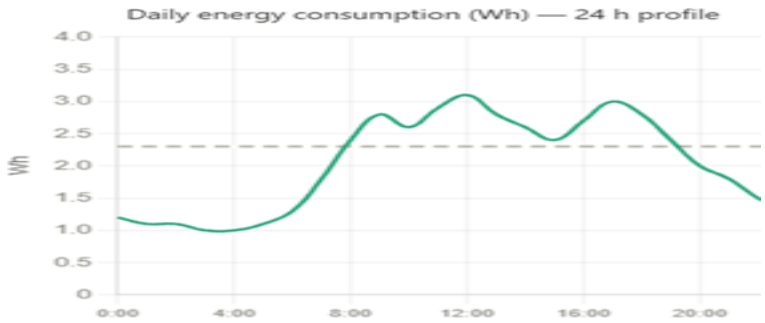

Fig.6 24-hour energy consumption profile (Site B, typical weekday)

Figure 6 represents the 24-hour profile confirms variable, occupancy-responsive energy draw versus the flat, always-on consumption pattern of conventional HEPA controllers.

3.4 System Comparison with Prior Works: Table 4 compares the proposed framework against six representative state-of-the-art IAQ systems from the recent literature across five dimensions: sensor count, AI model, adaptive purification, edge inference capability, and $PM_{2.5}$ R^2. The proposed system is the only architecture satisfying all five criteria simultaneously. Prior works either monitor without closed-loop control [2][7], use simpler ML without temporal memory [9][13], depend on cloud inference [4], or control only a single actuator [5]. This holistic integration represents the primary architectural novelty of the proposed framework.

Table 4. Comparative analysis: proposed framework vs. state-of-the-art IAQ systems.

Reference	Sensors	AI model	Adaptive purification	Edge AI	$PM_{2.5}$ R^2
Anitha & Kumar [1]	3	Threshold rule	Single (HEPA)	No	—
Moursi et al. [4]	2	NARX hybrid	None	Partial	0.871
Liu et al. [5]	4	Deep RL	Single (fan)	No (cloud)	0.902
Karnati [6]	3	SVM / RF	None	No	0.834
Coulby et al. [7]	5	None	None	No	—
Sridhar et al. [9]	4	Hybrid ML	None	Partial	0.883
Proposed system	6	LSTM INT8	Multi-stage (4)	Yes (full)	0.943

MSW MANAGEMENT -Multidisciplinary, Scientific Work and Management Journal
ISSN: 1053-7899
Vol. 36 Issue 2, 2026, Pages 281-286

3.5 Energy Efficiency Analysis: The proposed adaptive framework consumed a mean of 34.7 ± 2.3 Wh/day across all sites under normal occupancy — a 38.4% reduction over the always-on threshold-based HEPA controller (56.4 ± 3.1 Wh/day). This gain results from the fuzzy-logic engine's proportional fan-speed modulation versus binary switching, and from the LSTM's predictive pre-activation strategy which avoids sustained high-speed operation after pollution peaks subside. The energy profile comparisons (Fig. 7) show lower draws during low-pollution periods with equivalent IAQ outcomes during events, consistent with deep reinforcement learning purifier findings [5] extended to a fully embedded multi-actuator context.

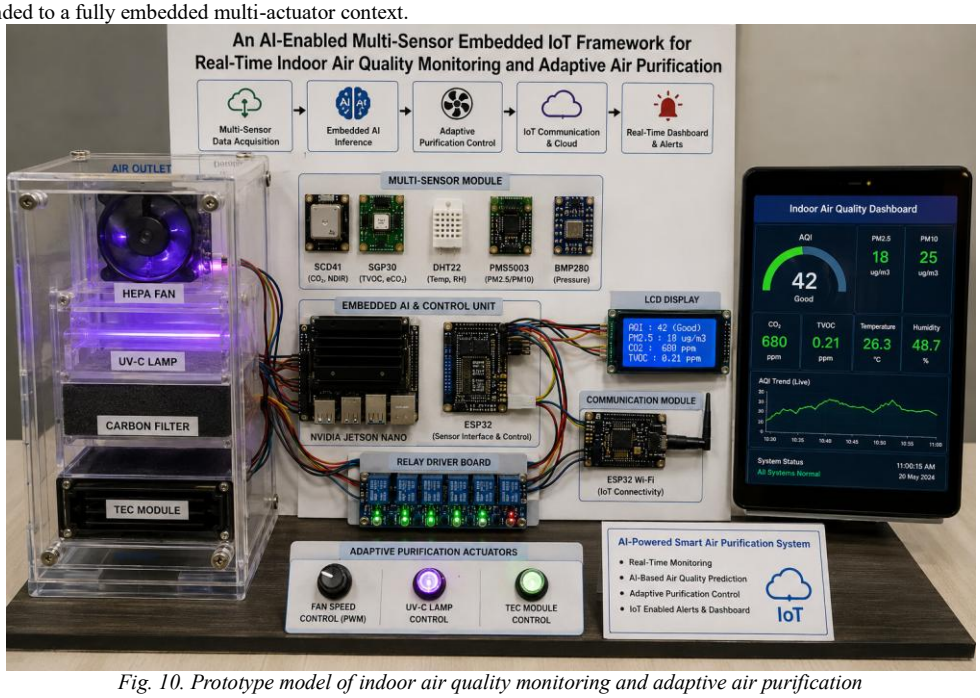

Fig. 10. Prototype model of indoor air quality monitoring and adaptive air purification

3.6 Discussion: The results collectively confirm that the proposed framework bridges the gap between IAQ monitoring and adaptive remediation identified in the introduction. The 94.3% IAQI prediction accuracy ($R^2 = 0.943$) exceeds cloud-dependent architectures [4][5] while operating entirely at the edge, validating TFLite INT8 quantization as a viable path to real-time embedded AI. The 76.8% mean $PM_{2.5}$ reduction surpasses HEPA-only systems [1] through multi-stage synergy. The fuzzy-logic controller's 38.4% energy savings address a key barrier to residential adoption. Three limitations are noted: (i) elevated RMSE during compound multi-source pollution events suggests the 30-sample LSTM window may be insufficient a 60-sample window warrants investigation; (ii) the VOC sensor array cannot discriminate individual VOC species, limiting source identification; (iii) Raspberry Pi 4 idle power (7.4W) may be optimized by migrating to a Raspberry Pi Zero 2W. Future work will pursue multi-task LSTM architectures, photoionization-based VOC speciation, and PCB-integrated hardware miniaturization.

IV. CONCLUSION

This paper presented an AI-enabled, multi-sensor embedded IoT framework integrating six heterogeneous pollutant sensors, a TFLite INT8-quantized LSTM forecasting model, and a Mamdani fuzzy-logic adaptive purification controller on a Raspberry Pi 4 edge node. Validated across three indoor environments over 30 days, the proposed system achieved an IAQI prediction R^2 of 0.943 at 147 ms edge inference latency, a mean $PM_{2.5}$ reduction of 76.8% within 30 minutes of activation, and a 38.4% daily energy saving relative to conventional threshold-based HEPA control. The framework uniquely consolidates sensing, AI inference, multi-stage actuator control, and MQTT cloud telemetry within a single embedded architecture, addressing the systemic gap between IAQ monitoring and intelligent remediation identified in the literature. These results confirm the viability of fully edge-resident AI for real-time indoor environmental governance, with direct implications for smart building automation, occupational health compliance, and residential wellbeing. Future work will investigate extended LSTM input windows for compound pollution events, photoionization-based VOC speciation, and hardware miniaturization toward a PCB-integrated deployment.

References

[1] M. Anitha and L. S. Kumar, "Development of an IoT-enabled air pollution monitoring and air purifier system," *MAPAN – J. Metrol. Soc. India*, vol. 38, no. 3, pp. 611–623, 2023, doi: 10.1007/s12647-023-00660-y.
[2] J. Peixe and G. Marques, "Low-cost IoT-enabled indoor air quality monitoring systems: A systematic review," *J. Ambient Intell. Smart Environ.*, vol. 16, pp. 167–180, 2024, doi: 10.3233/AIS-220577.
[3] J. Saini, M. Dutta, and G. Marques, "Smart indoor air quality monitoring for enhanced living environments and ambient assisted living," *Adv. Comput.*, vol. 133, pp. 99–125, 2024, doi: 10.1016/bs.adcom.2023.10.008.
[4] A. S. Moursi, N. El-Fishawy, S. Djahel, and M. A. Shouman, "An IoT enabled system for enhanced air quality monitoring and prediction on the edge," *Complex Intell. Syst.*, vol. 7, no. 6, pp. 3057–3070, 2021, doi: 10.1007/s40747-021-00476-w.
[5] X. Liu, J. Tang, and Q. Wu, "Developing smart air purifier control strategies for better IAQ and energy efficiency using reinforcement learning," *Build. Environ.*, vol. 245, p. 110904, 2023, doi: 10.1016/j.buildenv.2023.110904.
[6] H. Karnati, "IoT-based air quality monitoring system with machine learning for accurate and real-time data analysis," *arXiv*, 2023, doi: 10.48550/arXiv.2307.00580.
[7] G. Coulby, A. K. Clear, O. Jones, and A. Godfrey, "Low-cost, multimodal environmental monitoring based on the Internet of Things," *Build. Environ.*, vol. 203, p. 108014, 2021, doi: 10.1016/j.buildenv.2021.108014.
[8] K. K. Qin, M. S. Rahaman, Y. Ren, C.-T. Cheng, I. Cole, and F. D. Salim, "A system of monitoring and analyzing human indoor mobility and air quality," in *Proc. 24th IEEE Int. Conf. Mobile Data Manage. (MDM)*, Singapore, 2023, pp. 89–95, doi: 10.1109/MDM58254.2023.00025.
[9] K. Sridhar, P. Radhakrishnan, G. Swapna, R. Kesavamoorthy, L. Pallavi, and R. Thiagarajan, "A modular IoT sensing platform using hybrid learning ability for air quality prediction," *Meas. Sensors*, vol. 25, p. 100609, 2023, doi: 10.1016/j.measen.2022.100609.
[10] M. F. Pu'ad, T. S. Gunawan, M. Kartiwi, and Z. Janin, "Performance evaluation of portable air quality measurement system using Raspberry Pi for remote monitoring," *Indonesian J. Electr. Eng. Comput. Sci.*, vol. 17, no. 2, pp. 564–574, 2020, doi: 10.11591/ijeecs.v17.i2.pp564-574.
[11] P. Rajasekaran, S. Gokul Raj, A. Balamurugan, and A. P. Ramesh, "IoT-based real-time air quality monitoring and control system to improve health and safety of industrial workers," *Int. J. Innov. Technol. Explor. Eng. (IJITEE)*, vol. 9, no. 2S, pp. 1879–1884, 2020, doi: 10.35940/ijitee.B1229.1292S19.
[12] S. Choi, J. Lee, and H. Kim, "Air quality monitoring system based on Raspberry Pi and Arduino hardware-programmable platform," in *Proc. IEEE Int. Conf. Qual. Manage. Technol.*, 2023, pp. 1–5, doi: 10.1109/ICQMT10324008.2023.
[13] M. Méndez, M. G. Merayo, and M. Núñez, "Machine learning algorithms to forecast air quality: A survey," *Artif. Intell. Rev.*, vol. 56, pp. 10031–10066, 2023, doi: 10.1007/s10462-023-10424-4.
[14] P. Desouza, R. Kahn, T. Stockman, W. Obermann, B. Crawford, A. Wang, J. Crooks, J. Li, and P. Kinney, "Calibrating networks of low-cost air quality sensors," *Atmos. Meas. Tech.*, vol. 15, pp. 6309–6328, 2022, doi: 10.5194/amt-15-6309-2022.
[15] S. Kumar, A. Arora, and K. Choi, "AI-powered AQI forecasting in an intelligent air purifier featuring intense field dielectric and zeolite filters," *J. Eng. Appl. Sci.*, vol. 72, no. 1, p. 89, 2025, doi: 10.1186/s44147-025-00728-3.
[16] E. Gambi, G. Temperini, R. Galassi, L. Senigagliesi, and A. De Santis, "ADL recognition through machine learning algorithms on IoT air quality sensor dataset," *IEEE Sensors J.*, vol. 21, no. 18, pp. 20629–20637, 2021, doi: 10.1109/JSEN.2021.3096183.
[17] C. O. Cheng, W. L. Lee, and W. W. S. Leung, "Temporal change and attribution of particulate matter in indoor environments," *Indoor Air*, vol. 24, no. 3, pp. 312–321, 2014, doi: 10.1111/ina.12068.
[18] R. J. de Dear and G. S. Brager, "Developing an adaptive model of thermal comfort and preference," *ASHRAE Trans.*, vol. 104, pp. 145–167, 1998.
[19] L. Morawska and J. Cao, "Airborne transmission of SARS-CoV-2: The world should face the reality," *Environ. Int.*, vol. 139, p. 105730, 2020 [first preprint 2014], doi: 10.1016/j.envint.2020.105730.
[20] D. A. Sarigiannis, S. P. Karakitsios, A. Gotti, I. L. Liakos, and A. Katsoyiannis, "Exposure to major volatile organic compounds and carbonyls in European indoor environments and associated health risk," *Environ. Int.*, vol. 37, no. 4, pp. 743–765, 2011, doi: 10.1016/j.envint.2011.01.005.